Title	Risk-Averse Preventive Voltage Control of AC/DC Power Systems Including Wind Power Generation
Authors(s)	Rabiee, Abbas; Soroudi, Alireza; Keane, Andrew
Publication date	2015-10
Publication information	IEEE Transactions on Sustainable Energy, 6 (4): 1494-1505
Publisher	IEEE
Item record/more information	http://hdl.handle.net/10197/6740
Publisher's statement	(c) 2015 IEEE. Personal use of this material is permitted. Permission from IEEE must be obtained for all other users, including reprinting/ republishing this material for advertising or promotional purposes, creating new collective works for resale or redistribution to servers or lists, or reuse of any copyrighted components of this work in other works
Publisher's version (DOI)	10.1109/TSTE.2015.2451511

Risk-Averse Preventive Voltage Control of AC/DC Power Systems Including Wind Power Generation

Abbas Rabiee, *Member, IEEE,* Alireza Soroudi, *Member, IEEE,* and Andrew Keane, *Senior Member, IEEE*

***Abstract*—Preventive voltage control (PVC) deals with the alert state of power systems, where the system operates in a stable regime but loading margin (LM) is insufficient or some operational constraints have been violated. Hence, the aim of PVC is to ensure a desired LM (i.e. restoration of normal operation state), while minimizing the corresponding control costs. This paper proposes a new stochastic PVC (SPVC) model for power systems operation, taking into account the uncertainties of wind power generation. The uncertainty of wind power generation is handled using scenario based modeling approach. The risk associated with each objective function is handled using conditional value at risk. Voltage set-points of generation units, active power re-adjustment of predetermined generating units, load reduction of a predetermined load buses, along with the intermittent wind power generation, are employed as control measures in the proposed SPVC approach. Line-commutated converter high-voltage DC (LCC-HVDC) link constraints, doubly fed induction generators' (DFIGs) capability curves are also considered in the proposed SPVC approach. To illustrate the effectiveness of the proposed approach, it is applied on the IEEE 39-bus test system. The obtained results substantiate the applicability of the proposed SPVC model to ensure secure operation of AC/DC power systems with high penetration of offshore wind farms.**

***Index Terms*—Conditional value at risk (CVaR), high voltage direct current (HVDC), preventive voltage control (PVC), scenario based modeling, uncertainty, wind power.**

NOMENCLATURE

Sets:

NB	Set of system buses
NG	Set of generators
NB_G	Set of buses with generation units
NG_b	Set of generators connected to bus b
NG_{PVC}	Set of generators participating in PVC
NB_{PVC}	Set of load buses participating in PVC
NB_{ex}	Set of buses connected to external network

Indecises:

s	Scenario index
b	Bus index
i	Generator index
m	Rectifier($m = r$)/inverter($m = i$)

AC network's variables and parameters:

P_{G_i}/Q_{G_i}	Active/reactive power generation by i^{th} thermal generation unit
P_{L_b}/Q_{L_b}	Active/reactive load in bus b
$\hat{P_{G_i}}/\hat{Q_{G_i}}$	Active/reactive power generation by i^{th} thermal generation unit in loadability limit point
$\hat{P_{L_b}}/\hat{Q_{L_b}}$	Active/reactive load in bus b in loadability limit point
P_w/Q_w	Active/reactive power output of wind farm
$\mu_b^{P/Q}$	Cost of decreasing active/reactive demand at bus b.
$\mu_b^{Pex/Qex}$	Cost of active/reactive power purchased from external network at bus b.
$P_{L_b}^{fr}, Q_{L_b}^{fr}$	Forecasted active/reactive load in bus b
Y_{bj}/γ_{bj}	Magnitude/angle of bj^{th} element of Y_{bus}
P_w^r	Rated active power output of wind farm
$\mu_i^{Pg,up/dn}$	Re-dispatch cost of increasing/decreasing the generator's active power output in bus i.
$\mu_{i,s}^{Qg,up/dn}$	Re-dispatch cost of increasing/decreasing the generator's reactive power output in bus i.
$p_{l,s}/q_{l,s}$	Ratio of actual active/reactive power demand to the corresponding forecasted value in scenario s
$p_{w,s}$	Ratio of available wind power generation capacity to its rated capacity in scenario s
$P_{G_i}^{sch}/Q_{G_i}^{sch}$	Scheduled active/reactive power generation by i^{th} thermal unit
V_b/θ_b	Voltage magnitude/angle in bus b
$\hat{V_b}/\hat{\theta_b}$	Voltage magnitude/angle of bus b at loadability limit point.

HVDC variables:

P_{d_m}	Active power flowing through HVDC link
φ_m	Angle difference between the fundamental line current and line-to-neutral AC voltage
$R_{c,m}$	Commutation resistances
V_{d_m}	DC voltages at the HVDC terminals
I_d	DC current carried by the HVDC link
α_m	Ignition angle
V_{d0_m}	Ideal no-load voltage at the terminals
B_m	Number of series-connected bridges in a terminal
$R_{L,d}$	Resistance of HVDC cable
Q_{d_m}	Reactive power flowing into HVDC link
$B_{sh,m}$	Susceptance of HVDC shunt filters
T_m	Tap ratio of HVDC's transformer
V_m	Voltage magnitudes of the AC terminals of HVDC
Q_{sh_m}	VAR compensations at HVDC terminals

Risk associated variables:

η	Auxiliary variable to define CVaR
$\Re$	Conditional value at risk (CVaR)
Ξ	Expected value operator
π_s	Probability of occurrence in scenario s
β	Weighting factor to indicate the importance of expected value ($\beta = 1$) compared to risk value ($\beta = 0$)

I. INTRODUCTION

A. Background, Aims and Motivations

VOLTAGE stability is defined as the ability of a power system in maintaining proper voltages at load buses in normal operation and emergency conditions. This issue has been recently at the central point of attention due to various reasons such as growth of electrical energy demand, economic

A. Rabiee is with the Department of Electrical Engineering, Faculty of Engineering, University of Zanjan, Zanjan 45371-38111, Iran, (e-mail: rabiee@znu.ac.ir).

Alireza Soroudi and Andrew Keane are with the School of Electrical, Electronic and Communications Engineering, University College Dublin, (e-mail: alireza.soroudi@ucd.ie, andrew.keane@ucd.ie) The work of A. Soroudi was conducted in the Electricity Research Centre, University College Dublin, Ireland, which is supported by the Commission for Energy Regulation, Bord Gáis Energy, Bord na Móna Energy, Cylon Controls, EirGrid, Electric Ireland, EPRI, ESB International, ESB Networks, Gaelectric, Intel, SSE Renewables, UTRC and Viridian Power & Energy. A. Soroudi is funded through Science Foundation Ireland (SFI) SEES Cluster under grant number SFI/09/SRC/E1780.

and environmental constraints in expanding generation and transmission capacities, and market pressure to reduce operating costs. Moreover, the recent trends toward smart grids and also increasing share of renewable energy resources in many power systems, due to the environmental concerns and low marginal operating costs, have intensified the need for powerful approaches for power system security enhancement [1], [2]. Under such circumstances, there is possibility of voltage instability occurrence and therefore, it has to be considered as an integral part of power systems operation and planning studies [3]. It can be avoided by preventive voltage control (PVC) or by post-contingency corrective voltage control (CVC). The post-contingency CVC aims to restore voltage stability by directing the system into a new secure equilibrium point shortly after a severe contingency, such as the outage of a heavily loaded transmission line or transformer [4]. But, PVC is initiated in the condition that the system's loading margin (LM), is less than a desired value [5]. In this situation, PVC measures modify the operating point to an equilibrium point with a LM greater than the desired value, and hence, voltage security of the system ensured [5]. LM is defined as the distance from current operating point to the voltage collapse (or loadability limit) point [6].

A powerful tool is needed in order to handle the uncertainties of wind and demand values and quantify the potential risk at the first step. On the second step the system operator should try to minimize these undesired impacts simultaneously.

B. Literature Review

Nowadays offshore wind farms are developing in many countries, because the best locations for onshore wind farms are already developed. The offshore wind farms are commonly located far away from the onshore grid. If the distance is long or if the offshore wind farm is connected to a weak AC onshore grid, a high-voltage dc (HVDC) transmission system may be a more suitable choice than the conventional high-voltage AC transmission [7].

A common phenomenon which is likely to occur in practical power systems, is the shortage of LM during the peak load period due to heavy loading condition. Hence, dependable PVC actions such as re-adjustment of voltage controllers' set points, active/reactive generation re-dispatch, load curtailment in more vulnerable nodes are vital to restore sufficient LM. One of the main barriers in proper implementation of PVC, is the uncertainties associated with the forecasted system parameters. By increasing penetration of volatile renewable energy resources such as wind power generation, the most important uncertain parameters which directly affect the LM as well as the total costs are wind power generation and demand values [8], [9]. These uncertainties impose technical and economic risks on the system operator [10]. For example [8] addresses a methodology based on PV and QV analysis for probabilistic risk of voltage collapse. The uncertainty in the amount of generation provided by the renewable resources is considered by scenario based modelling. LM is considered as a stochastic variable in [9] and the impact of uncertain power injections by wind farms on the LM is investigated. In [11] an approach is proposed to increase wind power penetration by placing new wind generation at the strong buses from the voltage stability viewpoint. Voltage stability is evaluated by modal and QV analyses. In [12] a probabilistic framework is proposed which evaluates voltage/rotor angle stability in the presence of HVDC connected wind farms. The authors in [13] proposed a methodology for coordinating reactive output of wind generators with other reactive sources for voltage stability enhancement. They show that significant improvement in voltage stability margin can be obtained if the reactive power output of wind farms can be properly coordinated with other reactive power resources in the system.

It could be observed from the above literature survey that in the presence of severe uncertainties characterizing the voltage stability of the system, both technically and economically, is a critical issue. Since PVC actions impose significant costs to the system, reduction of these costs is desirable for system operator. Hence, it is necessary to characterize the voltage stability issue precisely, to make realistic decisions in which both technical and economic concerns are considered simultaneously.

TABLE I
COMPARING DIFFERENT MODELS WITH THE PROPOSED APPROACH

Reference	HVDC	Uncertainty	Risk	Voltage stability	Stochastic programming
[9]	N	Y	N	Y	N
[8]	N	Y	N	Y	N
[11]	N	N	N	Y	N
[12]	Y	Y	N	Y	N
[13]	N	N	N	Y	N
[14]	Y	N	N	N	N
[15]	Y	N	N	N	N
Proposed	Y	Y	Y	Y	Y

The proposed method tries to analyze the HVDC connected wind turbines considering the uncertainty and risk hedging issues. The voltage stability is enhanced using a stochastic programming technique.

C. Contributions

Table I summarizes a taxonomy of proposed methodologies for wind power integration in OPF. Hence, in this paper a new stochastic PVC (SPVC) model is proposed for operation of AC/DC power systems considering the uncertainty of wind power generation and demand values. Scenario based modeling is employed to properly handle these uncertainties. The aim of the proposed SPVC is to modify the operation point of the system in a way that for all probable scenarios, the system has sufficient LM and the cost of PVC controls is minimized. Also, it is assumed that wind power is supplied from an offshore site which is connected via a HVDC link to the AC onshore grid. In order to provide a SPVC which is both technically and economically efficient, conditional value at risk (CVaR) index is employed to determine the best strategy for system operators to cover the power demand uncertainties from different options in a secure way, especially form the LCC-HVDC connected uncertain offshore wind forms. Considering the CVaR in SPVC ensures that at in all probable scenarios, the required LM is ensured as well as the cost of PVC controls is reasonable. Hence, the proposed SPVC model gives a technical-economical decision making tool for power system operators.

The main contributions of this paper are listed as follows:

1) It provides a methodology to characterize both technical and economic issues of voltage stability.
2) The proposed method aims to reduce the associated technical and economic risks of PVC via CVaR index.
3) It considers the main sources of uncertainties, i.e. wind power generation and demand values, simultaneously. Hence, the proposed SPVC approach provides a realistic and practical decision making tool for system operator.
4) Since the new wind farms are constructed at the offshore sites and connected to the system via HVDC links, the proposed SPVC scheme considers the steady state model of such technology and formulate the voltage stability problem in the presence of offshore and HVDC-connected wind farms.
5) The proposed SPVC scheme, considers the LM as a stochastic variable which precisely models the system trajectory from the modified operation point to the collapse point in different probable scenarios. This treatment of system-wide voltage stability problem in the presence of uncertainties is not only considers the worst-case scenario but also other operating states.

D. Paper Organization

The rest of this paper is set out as follows: Section II presents a basic description of PVC. Section III deals with the uncertainty modeling and risk implementation in stochastic problems. Section IV presents formulation of the proposed SPVC problem. Case study and numerical results are given in Section V and finally, Section VI summarizes the findings and concludes the paper.

II. Description of PVC

According to the classification given in [16], operational states of practical power systems are as follows: Normal, Alert, Emergency, In Extremist and Restorative modes. The system is in Alert state if the operational constraints such as voltage/line-flow limits are violated or the security level of the system decreases below a certain threshold. In such a condition, preventive controls are activated manually or automatically, to restore the Normal state. One of the main criteria for addressing security of power systems, is the distance in MW (or MVar or MVA) from the current operating point to the maximum transmittable power point or voltage collapse point [17]- [18], which is called loading margin (LM). Voltage collapse occurs following a large disturbance or suddenly load increase in a heavily loaded power system. Control actions taken to prevent voltage instability prior to occurrence of contingencies or subject to the daily load changes are called preventive voltage control (PVC). For secure operation of a system, it is suggested to preserve specified LMs for both pre- and post-contingency states [18]. PVC deals with the situation in which the system operating point is stable but LM is less than the desired value. Accordingly, PVC actions are taken to ensure a desired LM. The control measures employed in PVC includes [5]:

- Active power re-dispatch of a pre-determined setting of fast generating units,
- Reactive power re-dispatch of dynamic VAR sources including generators, synchronous condensers, and FACTS controllers,
- Determination of on/off positions of capacitors/reactors,
- Determination of transformers tap and phase shifters set point,
- Load curtailment.

In Fig. 1, the base-case operating point A, (with the corresponding load P^0), is located on curve (1) with the corresponding loadability limit point A'. This point is stable, but with insufficient LM (i.e. $\lambda_0 < \lambda_{des}$). Following the PVC, loci of system's operation points will be modified to curve (2), and new secure operating point B with $\lambda = \lambda_1 \geq \lambda_{des}$ is obtained. λ_1 is calculated subject to the corresponding loadability limit point, i.e. B'.

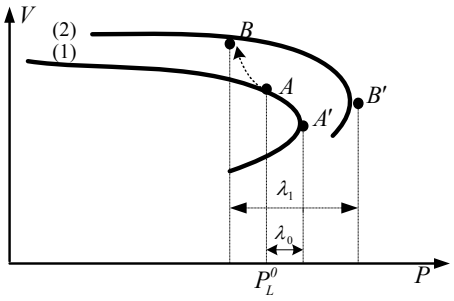

Fig. 1. The operation point evolution by execution of PVC

III. Uncertainty and Risk Modeling

In every engineering problem the decision maker tries to solve an optimization problem which contains some objective functions and some constraints. Usually the input parameters of such an optimization problem are subject to uncertainty. Depending on the nature of uncertainty, there are several techniques to model them such as Information gap decision theory [19], [20], fuzzy logic [21], robust optimization [22] and stochastic techniques. The stochastic techniques usually require the historic data of uncertain parameter. One of the well-known methods in stochastic techniques is the scenario based modeling. It is assumed that the probability density functions (PDF) of uncertain parameters are available. In scenario based modeling, the uncertain outcome set for uncertain parameter is discretized using its PDF. Each discrete event (Λ_s) is called a scenario with the known probability of occurrence (π_s). The conventional way of dealing with uncertainty using scenario based method is optimizing the expected value of (Λ_s) over the scenario set as follows.

$$\min / \max_{\bar{U}} \Xi_f(\bar{U}, \Lambda_s) \tag{1}$$

$$\Xi_f(\bar{U}, \Lambda_s) = \sum_s (\pi_s f(\bar{U}, \Lambda_s)) \tag{2}$$

$$\mathbf{H}_i(\bar{U}) \leq \bar{0}, i \in \Gamma \tag{3}$$

$$\bar{U} = \{\Psi, \Omega_s\} \tag{4}$$

Γ is the set of all constraints. In this framework, the decision variables include two sets of decisions Ψ, Ω_s. The first variable set (Ψ), represents the "**Here and now**" or "**First**

stage" decisions. These variables are set prior to realization of uncertain parameters and are independent of scenarios. The second variable set (Ω_s), represents the "**Wait and see**" or "**Second stage**"decisions. These variables are set posterior to realization of uncertain parameters and are dependent of scenarios. The whole decision making procedure is called the two stage decision making. Optimizing the expected value is not the best way to deal with uncertainties because without considering the risks of objective functions the decision maker may face undesired situations. There are several risk measures to handle the risks in scenario based uncertainty modeling and decision making like variance, shortfall probability, expected shortfall, value at risk and conditional value at risk (CVaR). In this paper, CVaR is chosen as the risk measure ($\Re$) to be optimized along with expected value because of its significant advantages over other risk measures, numerical efficiency and stability of calculations [23]. The procedure for maximization/minimization is as follows [24]:

$$\max_{\bar{U}} OF = \beta \Xi_f(\bar{U}, \Lambda_s) + (1-\beta)\Re \tag{5}$$

$$\Re = \eta - \frac{1}{1-\epsilon}\sum_s \pi_s \max(\eta - f(\bar{U}, \Lambda_s), 0) \tag{6}$$

$$\min_{\bar{U}} OF = \beta \Xi_f(\bar{U}, \Lambda_s) + (1-\beta)\Re \tag{7}$$

$$\Re = \eta + \frac{1}{1-\epsilon}\sum_s \pi_s \max(f(\bar{U}, \Lambda_s) - \eta, 0) \tag{8}$$

where $\Re$ is computed as the expected profit in the $(1-\epsilon)100\%$ worst scenarios. ϵ is indicating the upper/lower tail of the cost/benefit distribution in $\min / \max$ (7)/(5). Ξ_f is the expected value of objective function over scenarios. η is the value at risk which is a lower $\alpha-$percentile of random variable Λ.

IV. Problem formulation

The goal of the system operator is optimizing the expected values of two objective functions namely, minimizing the cost of preventive voltage control and maximizing the loading margin of each scenario while satisfying network's equality and inequality operational constraints. The assumptions, objectives, decision variables and constraints are described as follows.

It is worth mentioning that the content of sections IV-B, IV-C and IV-D are derived from well-established load flow and HVDC models which are given in [4], [15], [16], [25]–[28].

A. Objective functions

There are two objective functions (OFs) in the proposed probabilistic PVC framework, namely the expected value of loading margin (i.e. Ξ_{LM}), and the expected value of total cost of active/reactive power generation/consumption re-dispatch along with energy procurement cost from external network (or pool market), (i.e. Ξ_{TC}). These OFs are characterized as follows.

$$\Xi_{LM} = \sum_s \pi_s \lambda_s \tag{9}$$

$$\Xi_{TC} = \sum_s \pi_s TC(s) \tag{10}$$

$$\begin{aligned} TC(s) = & \sum_{i \in NG_{PVC}} \left(\mu_i^{Pg,up} \Delta P_{G_{i,s}}^{up} + \mu_i^{Pg,dn} \Delta P_{G_{i,s}}^{dn} \right) \\ & + \sum_{i \in NG} \left(\mu_{i,s}^{Qg,up} \Delta Q_{G_{i,s}}^{up} + \mu_{i,s}^{Qg,dn} \Delta Q_{G_{i,s}}^{dn} \right) \\ & + \sum_{i \in NB_{PVC}} \left(\mu_{b,s}^{P} \Delta P_{L_{b,s}} + \mu_{b,s}^{Q} \Delta Q_{L_{b,s}} \right) \\ & + \sum_{i \in NB_{ex}} \left(\mu_{b,s}^{Pex} P_{b,s}^{ex} + \mu_{b,s}^{Qex} Q_{b,s}^{ex} \right) \end{aligned} \tag{11}$$

Equation (9) is the expected value of LM which indicates that the average LM in all scenarios should be maximized which ensures sufficient distance from the voltage collapse point in all scenarios. Also, (10) is the expected cost of PVC actions which should be minimized. The PVC cost associated with each scenario is given in (11), where the first and second lines in the right hand side of (11) are active and reactive power generation re-dispatch costs, the third line is the cost of active and reactive load re-adjustment, and the last line is the cost of energy procurement from the external network to make an instantaneous balance between the generation and demand.

B. AC power flow constraints

The standard AC power flow constraints and operational limits are as follows [4], [25].

$$\sum_{i=1}^{NG_b} P_{G_{i,s}} - \left(P_{L_{b,s}} - \Delta P_{L_{b,s}}\right) = V_{b,s} \sum_j V_{j,s} Y_{bj} cos(\theta_{b,s} - \theta_{j,s} - \gamma_{bj}), \forall b \in NB \tag{12}$$

$$\sum_{i=1}^{NG_b} Q_{G_{i,s}} - \left(Q_{L_{b,s}} - \Delta Q_{L_{b,s}}\right) = V_{b,s} \sum_j V_{j,s} Y_{bj} sin(\theta_{b,s} - \theta_{j,s} - \gamma_{bj}), \forall b \in NB \tag{13}$$

$$P_{G_{i,s}} = \begin{cases} P_{G_i}^{sch} & \forall i \in NG_{PVC} \\ P_{G_i}^{sch} + \Delta P_{G_{i,s}}^{up} - \Delta P_{G_{i,s}}^{dn} & \forall i \in NG_{PVC}, \forall s \end{cases} \tag{14}$$

$$Q_{G_{i,s}} = Q_{G_i}^{sch} + \Delta Q_{G_{i,s}}^{up} - \Delta Q_{G_{i,s}}^{dn} \quad \forall i \in NG, \forall s \tag{15}$$

$$P_{G_i}^{min} \le P_{G_i} \le P_{G_i}^{max} \quad \forall i \in NG, \forall s \tag{16}$$

$$Q_{G_i}^{min} \le Q_{G_{i,s}} \le Q_{G_i}^{max} \quad \forall i \in NG, \forall s \tag{17}$$

$$0 \le \Delta P_{G_{i,s}}^{up} \le \Delta P_{G_i}^{up,max} \quad \forall i \in NG_{PVC}, \forall s \tag{18}$$

$$0 \le \Delta P_{G_{i,s}}^{dn} \le \Delta P_{G_i}^{dn,max} \quad \forall i \in NG_{PVC}, \forall s \tag{19}$$

$$0 \le \Delta Q_{G_{i,s}}^{up} \le \Delta Q_{G_i}^{up,max} \quad \forall i \in NG, \forall s \tag{20}$$

$$0 \le \Delta Q_{G_{i,s}}^{dn} \le \Delta Q_{G_i}^{dn,max} \quad \forall i \in NG, \forall s \tag{21}$$

$$P_{b,s}^{ex,min} \le P_{b,s}^{ex} \le P_{b,s}^{ex,max} \quad \forall b \in NB_{ex}, \forall s \tag{22}$$

$$Q_{b,s}^{ex,min} \le Q_{b,s}^{ex} \le Q_{b,s}^{ex,max} \quad \forall b \in NB_{ex}, \forall s \tag{23}$$

$$V_b^{min} \le V_{b,s} \le V_b^{max} \quad \forall b \in NB, \ \forall s \tag{24}$$

$$|S_{\ell,s}(V, \theta, s)| \le S_\ell^{max} \quad \forall \ell \in NL, \ \forall s \tag{25}$$

where, constraints (12), (13) are load flow equations of secure operation point (i.e. point B in Fig. 1), equations (14)-(21)

shows the re-dispatch possibility of active/reactive power generations and the corresponding limits, constraints (22), (23) are the limits on the exchanged active/reactive power between the system and the external network. Also, the limits on the voltage magnitudes and line flows are given by (24), (25).

In order to precisely characterize the LM, it is necessary to consider the power flow equations and operational limits for the corresponding loadability limit point (point B' in Fig. 1) as follows [26], [28].
$\forall b \in NB, \forall s$:

$$\sum_{i=1}^{NG_b} \hat{P}_{G_{i,s}} + P_{b,s}^{ex} - \hat{P}_{L_{b,s}} = \hat{V}_{b,s} \sum_j \hat{V}_{j,s} Y_{bj} cos(\hat{\theta}_{b,s} - \hat{\theta}_{j,s} - \gamma_{bj}) \quad (26)$$

$$\sum_{i=1}^{NG_b} \hat{Q}_{G_{i,s}} + Q_{b,s}^{ex} - \hat{Q}_{L_{b,s}} = \hat{V}_{b,s} \sum_j \hat{V}_{j,s} Y_{bj} sin(\hat{\theta}_{b,s} - \hat{\theta}_{j,s} - \gamma_{bj}) \quad (27)$$

$$\hat{P}_{L_{b,s}} = (1 + k_{L_b}\lambda_s) P_{L_{b,s}} \qquad \forall b \in NB, \forall s \quad (28)$$

$$\hat{Q}_{L_{b,s}} = (1 + k_{L_b}\lambda_s) Q_{L_{b,s}} \qquad \forall b \in NB, \forall s \quad (29)$$

$$\hat{P}_{G_{i,s}} = \min\left(P_{G_i}^{max}, (1 + k_{G_i}\lambda_s)\right) \qquad \forall i \in NG, \forall s \quad (30)$$

$$P_{G_i}^{min} \le \hat{P}_{G_i} \le P_{G_i}^{max} \qquad \forall i \in NG, \forall s \quad (31)$$

$$Q_{G_i}^{min} \le \hat{Q}_{G_{i,s}} \le Q_{G_i}^{max} \qquad \forall i \in NG, \forall s \quad (32)$$

$$V_b^{min} \le \hat{V}_{b,s} \le V_b^{max} \qquad \forall b \in NB, \forall s \quad (33)$$

$$\hat{V}_b = V_b + \nu_b^{dn} - \nu_b^{up}, \qquad \forall b \in NB_G \quad (34)$$

$$(Q_{G_{i,s}}^{max} - Q_{G_{i,s}})\nu_b^{up} \le 0 \ \forall i \in NB, \forall b \in NB_G, \forall s \quad (35)$$

$$(Q_{G_{i,s}} - Q_{G_{i,s}}^{min})\nu_b^{dn} \le 0 \ \forall i \in NB, \forall b \in NB_G, \forall s \quad (36)$$

$$\nu_b^{dn}, \nu_b^{up} \ge 0, \qquad \forall b \in NB_G \quad (37)$$

$$\lambda_s > 0 \quad \forall s \quad (38)$$

where, (26), (27) are load flow equations of loadability limit point, equations (28)-(29) are active/reactive loads at the loadability limit point, constraints (30)-(32) are active/reactive power generation at the loadability limit point and their corresponding limits. Also, the limits on the voltage magnitudes at the loadability limit point are given by (33). Besides, the constraints (34)-(37) ensure feasibility of the post-PVC operating point (point B in Fig. 1) and a trajectory from point B leading to point B' when the loads increment [26], [28]. Also, (38) guarantees a positive LM for all scenarios.

C. LCC-HVDC Model

The schematic of the LCC-HVDC link is depicted in Fig. 2. The HVDC connects the offshore wind farm to the AC network, and hence it is connected to the wind farm at its rectifier terminal, whereas it delivers the power produced by the farm to the AC system at its inverter side. The steady state power flow equations of the LCC-HVDC system are as follows [15], [16], [27]. In scenario s, and for $m = r, i$ (r: Rectifier, i: Inverter):

$$V_{d0_{m,s}} = \frac{3\sqrt{2}}{\pi} B_m T_m V_{m,s} \quad (39)$$

$$V_{d_{m,s}} = V_{d0_{m,s}} cos(\alpha_{m,s}) - B_m R_{c,m} I_{d,s} \quad (40)$$

$$I_{d,s} = \frac{V_{d_{r,s}} - V_{d_{i,s}}}{R_{L,d}} \quad (41)$$

$$cos(\varphi_{m,s}) = \frac{V_{d_{m,s}}}{V_{d0_{m,s}}} \quad (42)$$

$$P_{d_{m_s}} = V_{d_{m,s}} I_{d,s} \quad (43)$$

$$Q_{m,s} = P_{d_{m,s}} tan(\varphi_{m,s}) \quad (44)$$

where (39) gives the relationship between ideal no-load voltage at the DC sides of the LCC-HVDC link, and the AC sides voltages. Equation (40) is the actual voltages at both DC terminals due to the commutation overlap, and (41) is the DC current flowing through HVDC. Also, (42) is the power factors at the HV buses of HVDC link's AC sides. Constraints (43), (44) are the DC active powers (which are equal to AC active powers), and the reactive power absorbed by the HVDC link's AC terminals By neglecting the converters' losses, respectively.

D. Load Flow Equations at the Interface of AC/DC Networks

According to Fig. 2, at the inverter side of the HVDC link, the power balance equations of AC/DC networks are as follows [15], [27].

$$P_{G_{i,s}} + P_{d_{i,s}} - P_{L_{i,s}} = V_{i,s} \sum_j V_{j,s} Y_{ij} cos(\theta_{i,s} - \theta_{j,s} - \gamma_{ij}) \quad (45)$$

$$Q_{G_{i,s}} + B_{sh,i} V_{i,s}^2 + Q_{sh_{i,s}} - Q_{d_{i,s}} - Q_{L_{i,s}} = V_{i,s} \sum_j V_{j,s} Y_{ij} sin(\theta_{i,s} - \theta_{j,s} - \gamma_{ij}) \quad (46)$$

From Fig.2, at the rectifier side, by neglecting power losses of transformers connecting the wind farm to the HVDC terminal, the power balance equations of the AC/DC systems are as follows:

$$P_{d_{r,s}} = P_{w,s} \quad (47)$$

$$Q_{d_{r,s}} = Q_{w,s} + B_{sh,r} V_{r,s}^2 + Q_{sh_{r,s}} \quad (48)$$

where, for $m = r, i$:

$$Q_{sh_{m,s}}^{min} \le Q_{sh_{m,s}} \le Q_{sh_{m,s}}^{max} \quad (49)$$

Also, the DFIG-based wind farm power production limits are as follows:

$$0 \le P_{w,s} \le P_{w,s}^{avl} \quad (50)$$

$$Q_{w,s}^{min} \le Q_{w,s} \le Q_{w,s}^{max} \quad (51)$$

for connection of offshore DFIG-based wind farms to onshore AC power grids, installation of synchronous reactive power compensator at both Rectifier terminals of LCC-HVDC links is essential, because AC voltage source is necessary for proper commutation of thyristor valves. The compensator utilized for this aim is STATCOM [29], which can produce suitable three phase AC voltage at the Rectifier terminals, both in start-up and steady state operation of offshore wind

farms. If the offshore AC grid voltage is kept constant by STATCOM control, then the output active and reactive power of DFIGs can be set for particular rotor (wind) speed to affect a standard variable speed energy capture. In this paper, the reactive power compensator at both terminals of LCC-HVDC link is considered. Referring to Fig. 2 and equations. (46) and (48), it is evidently observed that the compensator is modelled as an AC voltage source which can produce $Q_{sh_{m,s}}$ at rectifier and inverter AC terminal. Hence, three phase AC voltage source is properly modelled.

E. Scenario based Uncertainty Modelling of Demand and Wind Power Generation

In this paper, a scenario based modeling is proposed to handle the uncertainty of demand and wind power generation [30]. In one hand, the system operator intended to perform PVC with the least imposed cost, and on the other hand, it is necessary to preserve a desired LM. Besides, since different scenarios of wind and demand are considered, it is possible to attain very high PVC cost or very small LM in some scenarios (i.e. risky decisions). Hence, the risk associated with each objective function (i.e. PVC cost and LM) should be considered properly in the proposed SPVC model. In order to do this, CVaR is utilized in this paper as follows

$$\min_{\bar{X}} OF_1 = \beta \Xi_f(\bar{X}, \Lambda_s) + (1-\beta)\Re_c \tag{52}$$

$$f(\bar{X}, \Lambda_s) = TC(s) \tag{53}$$

$$\Re_c = \eta_c + \frac{1}{1-\epsilon}\sum_s \pi_s \zeta_s^c \tag{54}$$

$$f(\bar{X}, \Lambda_s) - \eta_c \leq \zeta_s^c \tag{55}$$

$$0 \leq \zeta_s^c \tag{56}$$

The equations (52) to (56) are formulated and interpreted based on (7)-(8). In (52), OF_1 consists of two terms, where the first term is the expected cost of PVC ($\Xi_f(\bar{X}, \Lambda_s)$) in all possible scenarios, and the second term is the corresponding CVaR value ($\Re_c$) which is the index of risk. Finally, η_c is the value at risk for cost function.

$$\max_{\bar{X}} OF_2 = \beta \Xi_g(\bar{X}, \Lambda_s) + (1-\beta)\Re_{LM} \tag{57}$$

$$g(\bar{X}, \Lambda_s) = \lambda_s \tag{58}$$

$$\Re_{LM} = \eta_{LM} - \frac{1}{1-\epsilon}\sum_s \pi_s \zeta_s^{LM} \tag{59}$$

$$\eta_{LM} - g(\bar{X}, \Lambda_s) \leq \zeta_s^{LM} \tag{60}$$

$$0 \leq \zeta_s^{LM} \tag{61}$$

The equation (57) is formulated and interpreted based on (5)-(6). Also, OF_2 in (57) composed of two terms, in which the first term is the expected value of LM in all possible scenarios ($\Xi_g(\bar{X}, \Lambda_s)$), and the second term (i.e. $\Re_{LM}$) is its corresponding CVaR value which is the measure of risk. Besides, η_{LM} in (60) is the value at risk for LM.

Hence, the overall OF to be minimized is defined as the weighted sum of the above risk constrained OFs as follows.

$$OF = w\frac{OF_1 - OF_1^{max}}{OF_1^{max} - OF_1^{min}} + (1-w)\frac{OF_2 - OF_2^{min}}{OF_2^{min} - OF_2^{max}} \tag{62}$$

It is worth noting that OF_1 should be minimized contrarily to OF_2. Hence, (62) is formulated in a way that minimizing the overall OF corresponds to minimization of OF_1 and maximization of OF_2, simultaneously.

F. Decision Variables

The decision variables of the proposed probabilistic PVC model include: Active power re-dispatch of pre-determined set of generation units, terminal voltage set point of all generator buses, tap position of load tap changers, active power generation of wind farm, reactive power injections at both terminals along with the tap settings of on-load tap changers of HVDC links. The proposed robust decision making framework finds the optimal values for these variables considering the uncertainty of wind power generation outputs. The sets of control, state and dependent variables are described as follows.

$$\bar{U} = \begin{bmatrix} \lambda_s & \forall s \\ V_b, \nu_b^{dn}, \nu_b^{up} & \forall b \in NB_G \\ T_{m,s} & \forall m = r, i \\ P_{w,s} & \forall s \\ Q_{sh_{m,s}} & \forall m = r, i, \forall s \\ \Delta P_{G_{i,s}}^{up}, \Delta P_{G_{i,s}}^{dn} & \forall i \in NG_{PVC}, \forall s \\ \Delta P_{L_{b,s}}^{up}, \Delta P_{L_{b,s}}^{dn} & \forall b \in NB_{PVC}, \forall s \end{bmatrix} \tag{63}$$

$$\bar{X} = \begin{bmatrix} V_b, \hat{V}_b & \forall b \notin NB_G \\ \theta_b, \hat{\theta}_b & \forall b \in NB \\ V_{d_{m,s}}, P_{d_{m,s}} & \forall m = r, i, \forall s \\ I_{d,s} & \forall s \end{bmatrix} \tag{64}$$

$$\bar{Y} = \begin{bmatrix} Q_{G_i}, \hat{P}_{G_i}, \hat{Q}_{G_i} & \forall i \in NG \\ S_\ell(V, \theta, s) & \forall \ell \in NL, \forall s \end{bmatrix} \tag{65}$$

V. Case Study and Numerical results

The proposed probabilistic PVC model is implemented and examined on the New-England 39 bus test systems. The single line diagram of this system is depicted in Fig. 2, and its data are presented in [31]. The initial operating point is also given in [31]. It is assumed that the very short term load forecast is 8% higher than the base-case load level given in [31]. For this load level, LM is very low and the system is in alert operation state. Thus, the PVC is activated to restore normal operation condition, by means of available control measures. In order to determine the LM in each scenario, the loads are increased evenly with $k_{L_b} = 1$. Also, active power output of the generators, not hitting their upper generation limits in the base-case, are also increased evenly with $k_{G_i} = 1$.

The cost coefficients of generators and demands (in \$/MW) to alter their scheduled productions and consumptions have been selected close to the corresponding locational marginal prices (LMPs) values [32]. It is assumed that adjusting the power production up is slightly more expensive than adjusting down the power production for generators [32]. Also, since only adjusting down is allowed in this model for loads, the corresponding cost is assumed to be slightly higher than the corresponding LMP.

The LMPs for this system in different scenarios are given in Tables X and XI (in the Appendix) for nodal active and reactive power injections. These values have been obtained

by MATPOWER [31]. Hence the cost of adjusting up for generators and adjusting down for loads (given in eq. (11)) are assumed to be 5% higher that the corresponding LMP. Also, the cost of power purchased from external network is also treated as the adjusting up cost of generators. Similarly, for adjusting down of power generation, the costs are assumed to be 0.95% of the corresponding LMP.

The generation units located at the following buses are selected by ISO for active power re-dispatch in PVC scenarios: 30, 31, 35, 37, 39. Besides, the following buses are permitted to utmost 20% active/reactive power demand reduction: 4, 8, 15, 16, 20, 21, 29, 39. Also, it is assumed that according to a contract between the ISO and an external network, the maximum amount of active and reactive power import to the network is 600 MW and 400 MVAr, respectively. The system is connected to the external network through bus 25, as depicted in Fig. 2.

In this study, an offshore wind farms is considered, with the capacity of 1000 MW. As it is depicted in Fig 2, it is connected to the AC system through bus 16, via a 24-pulse LCC-HVDC link. HVDC link is bipolar with the rating of 1000 MW and 250 kV. The data of this DC links derived from [27].

Using the technique described in [22], the PDF of wind speed is divided into several intervals, and the probability of falling into each interval is calculated. A mean value is also assigned for each interval which is indicator of the corresponding interval. Demand values are also modeled using a normal PDF with a known mean and variance (which is available from load forecasting unit). It is assumed that the load and wind power generation scenarios are independent so the scenarios are combined to construct the whole set of scenarios as follows.

$$\pi_s = \pi_l \times \pi_w \tag{66}$$

where π_l and π_w are the probabilities of l-th load and w-th wind scenarios, respectively. Hence, total number of scenarios, is $n_l \times n_w$, where n_l and n_w are the number of individual load and wind scenarios. If the number of scenarios are too high then some scenario reduction techniques [33] can be applied to the problem.

In this work, three scenarios are considered for load by using the normal distribution. The mean value of load in each bus, is its forecasted value and the standard deviation is assumed to be 2% of the corresponding mean value. Also, three scenarios are considered for wind power generation, which the probability of all individual scenarios are given in Table II. It should be noted that finding the scenarios which describe all states of wind power generation depends on the wind farm location. Some techniques have been reported in the literature to find these states and the associated probabilities (which are based on the historical data and measurements) [34]. In other words, there is no general table for describing the wind power states (or scenarios). By incorporating these scenarios using (66), 9 mixed wind-load scenarios are attained which are given in Table III.

Active and reactive loads in bus b, as well as the available wind power at scenario s are calculated as follows.

$$P_{L_{b,s}} = p_{l,s} \times P^{fr}_{L_b} \tag{67}$$

$$Q_{L_{b,s}} = q_{l,s} \times Q^{fr}_{L_b} \tag{68}$$

$$P^{avl}_{w,s} = p_{w,s} \times P^{r}_{w} \tag{69}$$

TABLE II
THE WIND AND DEMAND SCENARIOS AND CORRESPONDING PROBABILITIES

Individual wind/load scenario	Percent (to nominal)	Probability
w_1	75	0.10
w_2	85	0.80
w_3	100	0.10
l_1	98	0.15
l_2	100	0.70
l_3	102	0.15

TABLE III
COMBINED WIND AND DEMAND SCENARIOS AND CORRESPONDING PROBABILITIES

Scenario	$p_{l,s}$	$p_{w,s}$	π_s
s_1	0.98	1.00	0.015
s_2	1.00	1.00	0.070
s_3	1.02	1.00	0.015
s_4	0.98	0.85	0.120
s_5	1.00	0.85	0.560
s_6	1.02	0.85	0.120
s_7	0.98	0.75	0.015
s_8	1.00	0.75	0.070
s_9	1.02	0.75	0.015

It is also assumed that in scenario s, $q_{l,s} = p_{l,s}$. The proposed probabilistic PVC model is implemented in General Algebraic Modeling System (GAMS) environment, and solved by SNOPT solver [35]. The probabilistic PVC is solved for different risk levels and weighting factors of the aforementioned objective functions. Table IV gives the obtained results for different values of β and w. In this study two extreme cases are investigated in detail, namely risk neutral strategy (without concerning about risk, i.e. for $\beta = 1$), and risk averse strategy (with fully concerning about risk, i.e. for $\beta = 0$). In both cases, the optimal settings of both "here and now" and "wait and see" control variables are presented.

TABLE IV
SOLUTION SUMMARY FOR DIFFERENT RISK LEVELS AND OFS' WEIGHTS

Sol_n	β	w	$\Re_c$(\$)	Ξ_c(\$)	$\Re_{LM}$	Ξ_{LM}	OF_1(\$)	OF_2
Sol_1		0.00	31653.831	28402.473	0.265	0.265	31653.831	0.265
Sol_2		0.25	28246.079	28205.194	0.265	0.265	28246.079	0.265
Sol_3	0.00	0.50	18108.682	18039.432	0.219	0.219	18108.682	0.219
Sol_4		0.75	679.361	677.734	0.043	0.043	679.361	0.043
Sol_5		1.00	34.080	32.643	0.013	0.013	34.080	0.013
Sol_6		0.00	29738.478	28522.174	0.264	0.265	29434.402	0.265
Sol_7		0.25	28239.334	28195.289	0.265	0.265	28228.323	0.265
Sol_8	0.25	0.50	17502.671	17449.000	0.214	0.214	17489.253	0.214
Sol_9		0.75	660.198	658.830	0.042	0.042	659.856	0.042
Sol_{10}		1.00	21.667	20.545	0.012	0.014	21.386	0.012
Sol_{11}		0.00	29676.899	28366.306	0.265	0.265	29021.603	0.265
Sol_{12}		0.25	28238.107	28197.459	0.265	0.265	28217.783	0.265
Sol_{13}	0.50	0.50	17173.122	17102.580	0.211	0.211	17137.851	0.211
Sol_{14}		0.75	660.329	658.827	0.043	0.043	659.578	0.043
Sol_{15}		1.00	20.154	19.123	0.008	0.009	19.639	0.009
Sol_{16}		0.00	30239.666	28732.855	0.258	0.258	29109.558	0.258
Sol_{17}		0.25	28260.782	28219.531	0.265	0.265	28229.843	0.265
Sol_{18}	0.75	0.50	17444.345	17365.582	0.214	0.214	17385.272	0.214
Sol_{19}		0.75	670.328	666.089	0.042	0.042	667.149	0.042
Sol_{20}		1.00	42.127	40.462	0.008	0.008	40.878	0.008
Sol_{21}		0.00	29126.508	28342.930	0.265	0.265	28342.930	0.265
Sol_{22}		0.25	29126.547	28205.435	0.265	0.265	28205.435	0.265
Sol_{23}	1.00	0.50	6400.742	4345.783	0.099	0.105	4345.783	0.105
Sol_{24}		0.75	1179.032	680.892	0.042	0.042	680.892	0.042
Sol_{25}		1.00	446.388	59.055	0.000	0.012	59.055	0.012

A. Risk neutral (RN) strategy (when $\beta = 1$)

Using the technique described in [36], the satisfaction level of each objective function is calculated and described in Table V. It is observed from this table that the best compromise solution in this strategy is Sol_{23}. For this optimal solution, the expected total cost and the expected LM are $4345.783 and

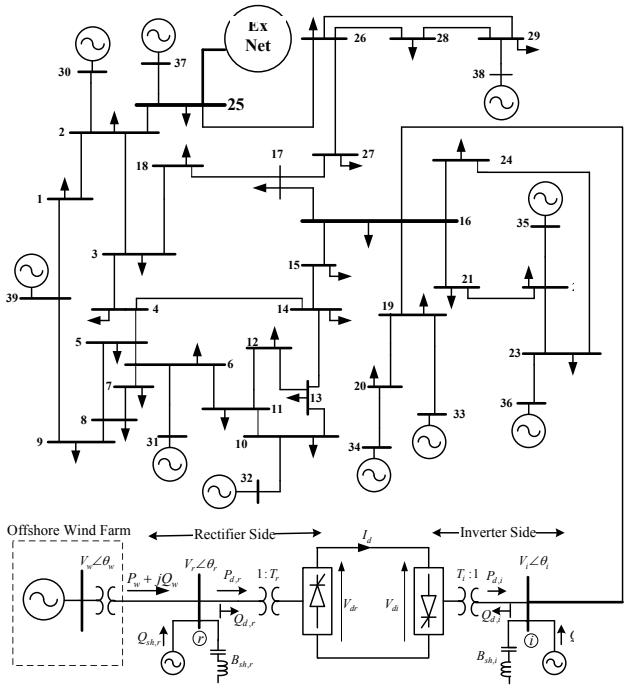

Fig. 2. Single line diagram of the network under study

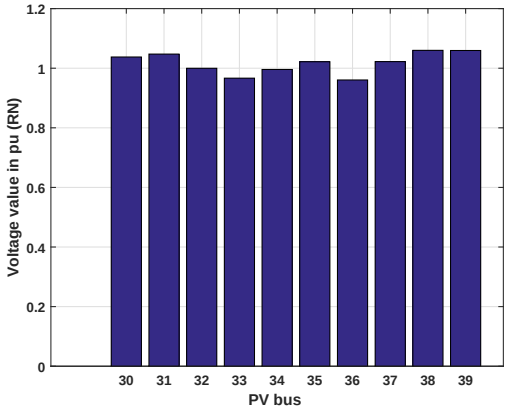

Fig. 3. Generator bus voltages (in pu), in RN strategy

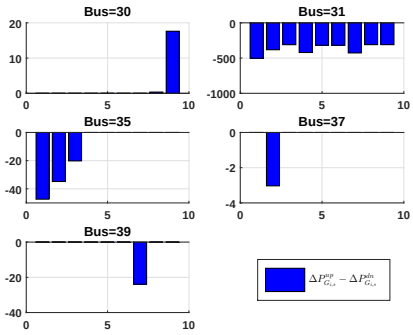

Fig. 4. Active power generation re-dispatch (in MW), in RN strategy. The horizontal axis shows the scenarios.

0.105, respectively. Also, the optimal re-dispatch of generation units are given in Fig. 3 for this solution. Besides, the values of active power generation re-dispatch of the generation units participating in PVC are presented in Fig. 4.

Active and reactive power outputs of the wind farm in all scenarios ($s_1 - s_9$) are given in Fig. 5. Besides, Fig. 6 shows reactive power purchased from external network (e.g. pool market) in all scenarios for this solution. It is observed from this figure that the purchased power in Scenario s_9 is much higher than other scenarios, because in this scenario the the demand is 2% greater than the expected value and the available capacity of wind farm is 75% of its nominal value. Also, optimal schedules of active/reactive load reduction at the buses participating in PVC program are depicted in Fig. 7. Besides, the optimal schedule of the HVDC connection for all scenarios are summarized in Table VI. The optimal tap ratios of transformers at both rectifier and inverter sides of the HVDC are as follows: $T_r = 0.515pu$ and $T_i = 0.483pu$.

TABLE V
OBJECTIVE FUNCTIONS VALUES AT THE RN STRATEGY ($\beta = 1$)

Sol_n	w	$OF_1(\$)$	OF_2	μ_{OF_1}	μ_{OF_2}	$\min(\{\mu_{OF_1}, \mu_{OF_2}\})$
Sol_{21}	0.00	28342.930	0.265	0.000	1.000	0.000
Sol_{22}	0.25	28205.435	0.265	0.005	0.999	0.005
Sol_{23}	**0.50**	**4345.783**	**0.105**	**0.848**	**0.375**	**0.375**
Sol_{24}	0.75	680.892	0.042	0.977	0.132	0.132
Sol_{25}	1.00	59.055	0.012	0.999	0.015	0.015

B. Risk averse (RA) strategy (when $\beta = 0$)

In this case, the risks associated with both objective functions are fully considered. Table VII gives the satisfaction level of each objective function for different values of weights (i.e. w). It is evidently observed from this table that in this case solution Sol_3 is dominated and it is the optimal compromise solution with the expected total cost and the expected LM equal to $\$18108.682$ and 0.219, respectively. Therefore, in this section the optimal settings of control variables are given for this solution. The optimal settings of generator bus voltages are given in Fig. 8. Also Fig. 9 illustrates active power re-dispatch of generators participate in the PVC.

Active and reactive power outputs of the wind farm connected to bus 16 for different scenarios are also given in Fig. 10. Besides, Fig. 6 shows reactive power purchased from external network, (e.g. pool market), in all scenarios. Active/reactive load reduction at the selected buses in all scenarios are depicted in Fig. 11. Table VIII gives the optimal schedule of HVDC link in all scenarios for this solution. Also, in this case, the optimal values of tap ratios at both AC sides of the HVDC link are as follows: $T_r = 0.523pu$ and $T_i = 0.491pu$.

TABLE VII
OBJECTIVE FUNCTIONS VALUES AT THE RA STRATEGY ($\beta = 0$))

Sol_n	w	$OF_1(\$)$	OF_2	μ_{OF_1}	μ_{OF_2}	$\min(\{\mu_{OF_1}, \mu_{OF_2}\})$
Sol_1	0.00	31653.831	0.265	0.000	1.000	0.000
Sol_2	0.25	28246.079	0.265	0.108	0.999	0.108
Sol_3	**0.50**	**18108.682**	**0.219**	**0.428**	**0.829**	**0.428**
Sol_4	0.75	679.361	0.043	0.978	0.161	0.161
Sol_5	1.00	34.080	0.013	0.998	0.049	0.049

TABLE VI
SCHEDULE OF HVDC LINK AT THE OPTIMAL RN STRATEGY

$Scenario\#$	$\varphi_r(Rad)$	$\varphi_i(Rad)$	$\alpha_r(Rad)$	$\alpha_i(Rad)$	$V_{d_r}(kV)$	$V_{d_i}(kV)$	$P_{d_r}(MW)$	$P_{d_i}(MW)$	$Q_{d_r}(MVAr)$	$Q_{d_i}(MVAr)$	$I_d(kA)$	$V_r(kV)$	$V_i(kV)$
s_1	0.312	0.287	0.155	0.080	492.944	477.265	386.453	374.161	124.746	110.580	0.784	214.886	214.886
s_2	0.328	0.343	0.080	0.110	491.560	469.838	533.892	510.299	181.834	182.301	1.086	215.424	215.424
s_3	0.373	0.413	0.119	0.200	484.110	457.433	645.749	610.164	252.417	267.273	1.334	215.629	215.629
s_4	0.449	0.441	0.350	0.335	466.630	450.000	387.999	374.171	186.984	176.733	0.831	214.886	214.886
s_5	0.328	0.343	0.080	0.110	491.560	469.837	533.892	510.299	181.835	182.302	1.086	215.424	215.424
s_6	0.361	0.401	0.080	0.177	486.265	459.720	645.387	610.156	243.715	258.896	1.327	215.629	215.629
s_7	0.312	0.287	0.155	0.080	492.944	477.265	386.453	374.161	124.746	110.580	0.784	214.886	214.886
s_8	0.328	0.343	0.080	0.110	491.560	469.838	533.892	510.299	181.834	182.301	1.086	215.424	215.424
s_9	0.361	0.401	0.080	0.177	486.265	459.720	645.387	610.156	243.715	258.896	1.327	215.629	215.629

TABLE VIII
SCHEDULE OF HVDC LINK AT THE OPTIMAL RA STRATEGY

$Scenario\#$	$\varphi_r(Rad)$	$\varphi_i(Rad)$	$\alpha_r(Rad)$	$\alpha_i(Rad)$	$V_{d_r}(kV)$	$V_{d_i}(kV)$	$P_{d_r}(MW)$	$P_{d_i}(MW)$	$Q_{d_r}(MVAr)$	$Q_{d_i}(MVAr)$	$I_d(kA)$	$V_r(kV)$	$V_i(kV)$
s_1	0.350	0.307	0.350	0.307	465.362	465.362	0.000	0.000	0.000	0.000	0.000	208.754	208.754
s_2	0.197	0.152	0.149	0.081	486.229	482.848	82.181	81.610	16.370	12.539	0.169	208.916	208.916
s_3	0.291	0.297	0.216	0.223	475.727	467.908	186.003	182.946	55.762	56.037	0.391	209.280	209.280
s_4	0.189	0.080	0.189	0.080	486.575	486.575	0.000	0.000	0.000	0.000	0.000	208.754	208.754
s_5	0.196	0.152	0.148	0.080	486.276	482.896	82.181	81.610	16.328	12.485	0.169	208.916	208.916
s_6	0.397	0.404	0.343	0.350	458.081	450.000	185.087	181.822	77.529	77.698	0.404	209.280	209.280
s_7	0.211	0.124	0.211	0.124	484.384	484.384	0.000	0.000	0.000	0.000	0.000	208.754	208.754
s_8	0.196	0.152	0.148	0.080	486.276	482.896	82.181	81.610	16.328	12.485	0.169	208.916	208.916
s_9	0.209	0.214	0.080	0.090	485.875	478.224	185.873	182.946	39.352	39.720	0.383	209.280	209.280

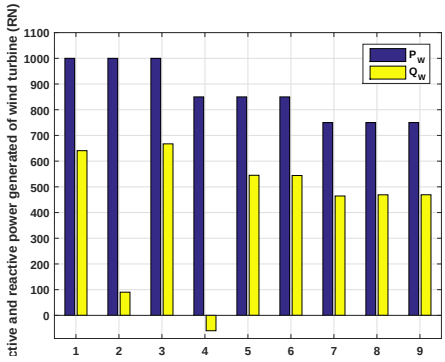

Fig. 5. Active/reactive power output (in MW/MVAr) of wind farm, in RN strategy.

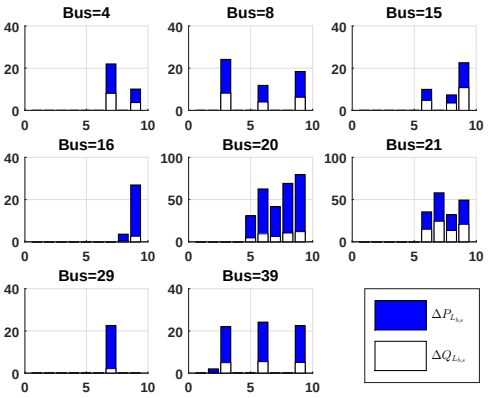

Fig. 7. Active (MW) and reactive (MVAr) load reduction, in RN strategy. The horizontal axis shows the scenarios.

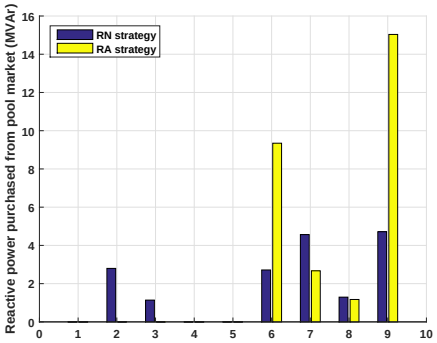

Fig. 6. Purchased reactive power (in MVAr) from external network, in RN/RA strategy.

C. Discussion on the obtained results

At the above two sections the optimal values of control variables have been proposed in terms of "First stage" control variables (such as generator bus voltages, tap ratios of HVDC's transformers), and "Second stage" control variables (such as wind farm's active/reactive power output, load reduction, active power generation re-dispatch and power purchased from external network).

In RN strategy, the probabilistic PVC is solved without concerning about the risks associated with each objective function, and hence it is a risky decision making strategy. In RA strategy, the corresponding risk of each objective function is considered and hence the results obtained from PVC are risk averse. Table IX summarizes the expected values of LM, TC, active/reactive load reduction and power purchased from the external network, along with the power output of wind farm. The following results are deducible from this table.

- By comparing RN and RA strategies, it is observed that in the RN solution, the expected TC is much less than the corresponding value in the RA attitude. It means that considering risk in decision making process, leads to conservative decision with higher control cost.
- At the RA strategy, the expected LM is much higher than the corresponding value at the RN strategy, which is due to the inclusion of the risk through CVaR constraints.
- It is observed that in RA strategy a slightly less wind

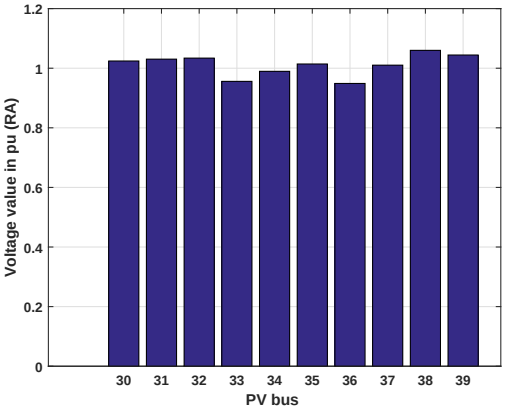

Fig. 8. Generator bus voltages (in pu), in RA strategy.

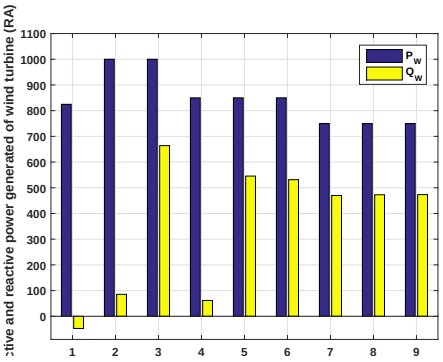

Fig. 10. Active/reactive power output (in MW/MVAr) of wind farm, in RA strategy.

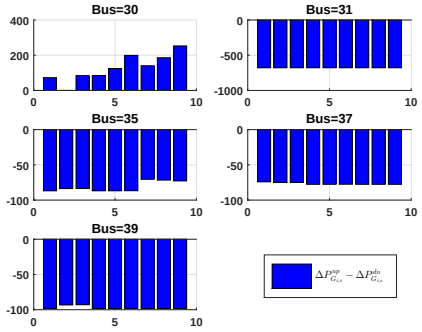

Fig. 9. Active power generation re-dispatch (in MW), in RA strategy. The horizontal axis shows the scenarios.

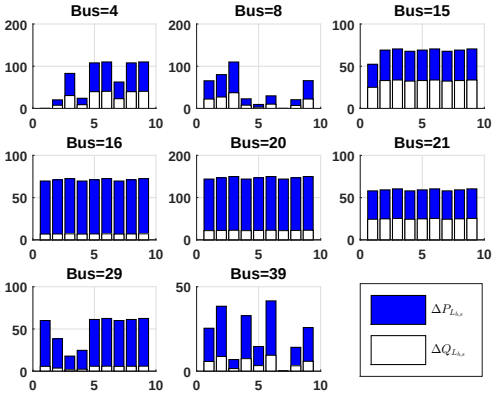

Fig. 11. Active (MW) and reactive (MVAr) load reduction, in RA strategy. The horizontal axis shows the scenarios.

power generation is scheduled in comparison with the RN strategy, which means that considering the risk does not affect the utilization of renewable energies. Besides, it is observed that in RA strategy more load curtailment is required.

Finally, it is observed that inclusion of risk in PVC leads to a solution with higher LM level (more volage stability margin), but with the expense of higher control costs.

TABLE IX
COMPARISON OF EXPECTED VALUES OF "SECOND STAGE" CONTROL VARIABLES

Variable	RN	RA
TC ($)	4345.783	18039.432
LM	0.105	0.219
$P^{ex}(MW)$	0.000	0.000
Q^{ex} (MVaR)	0.769	1.469
P_{rd} (MW)	51.126	534.215
Q_{rd} (MVaR)	11.802	137.578
P_w (MW)	855.000	852.370
Q_w (MVaR)	436.084	439.092

VI. CONCLUSION

In this paper a stochastic model is proposed for preventive voltage control (PVC) in AC/DC power systems. The LCC-HVDC link is employed to connect offshore wind farm to the rest of AC IEEE 39-bus test system. The main conclusions are summarized as follows:

- The uncertainties of wind power generation and demand are handled using scenario based uncertainty modelling approach. This would allow the decision maker to avoid unwanted circumstances (increasing cost / decreasing the LM). The conditional value at risk (CVaR) is used as the risk measure.
- Various control variables such as generator bus voltages, tap ratios of HVDC connecting transformers, active/reactive power generation re-dispatch, load curtailment, power generation of wind farm along with power purchased from external network are considered in the proposed stochastic model of PVC. Some of these variables are "'first stage"' variables (do not change in various scenarios) and the rest of them are "'second stage"' decision variables (change in different scenarios).
- The expected LM is maximized while minimizing the corresponding control costs for different levels of risk associated with each objective function.
- The risk averse strategy leads to a solution with higher LM level (i.e. more distance to voltage collapse), but with

TABLE X
LMPS FOR NODAL ACTIVE POWERS IN DIFFERENT SCENARIOS ($/MWH)

Bus	s1	s2	s3	s4	s5	s6	s7	s8	s9
B1	11.304	11.605	11.907	11.401	11.700	12.000	11.624	11.923	12.223
B2	11.090	11.386	11.680	11.116	11.401	11.688	11.337	11.623	11.909
B3	11.126	11.424	11.722	11.164	11.454	11.744	11.391	11.681	11.971
B4	10.972	11.249	11.531	11.211	11.502	11.795	11.437	11.729	12.021
B5	10.965	11.240	11.519	11.219	11.510	11.802	11.443	11.734	12.026
B6	10.943	11.216	11.495	11.202	11.492	11.783	11.425	11.715	12.006
B7	11.019	11.297	11.580	11.270	11.564	11.858	11.495	11.788	12.082
B8	11.049	11.329	11.613	11.296	11.591	11.887	11.521	11.816	12.111
B9	11.227	11.518	11.813	11.411	11.710	12.010	11.635	11.934	12.234
B10	10.819	11.083	11.354	11.113	11.399	11.685	11.335	11.621	11.908
B11	10.861	11.129	11.402	11.144	11.432	11.720	11.366	11.654	11.942
B12	10.841	11.106	11.378	11.136	11.423	11.711	11.359	11.646	11.934
B13	10.818	11.081	11.352	11.125	11.412	11.699	11.348	11.635	11.923
B14	10.806	11.068	11.337	11.148	11.437	11.726	11.375	11.664	11.953
B15	10.469	10.699	10.944	11.059	11.346	11.634	11.293	11.581	11.869
B16	10.262	10.476	10.707	10.957	11.240	11.524	11.193	11.477	11.762
B17	11.180	11.497	11.808	11.035	11.321	11.607	11.268	11.554	11.840
B18	11.173	11.484	11.790	11.099	11.387	11.675	11.329	11.617	11.906
B19	10.170	10.379	10.606	10.843	11.123	11.403	11.073	11.354	11.635
B20	10.196	10.406	10.635	10.868	11.151	11.435	11.099	11.383	11.667
B21	10.229	10.441	10.671	10.915	11.196	11.477	11.149	11.430	11.712
B22	10.157	10.365	10.591	10.832	11.108	11.384	11.062	11.338	11.615
B23	10.158	10.367	10.592	10.833	11.109	11.385	11.062	11.339	11.615
B24	10.265	10.479	10.710	10.958	11.241	11.525	11.194	11.478	11.762
B25	10.866	11.155	11.441	10.871	11.146	11.422	11.085	11.359	11.634
B26	11.085	11.389	11.689	11.015	11.297	11.580	11.237	11.519	11.802
B27	11.162	11.473	11.780	11.058	11.344	11.630	11.286	11.571	11.858
B28	11.086	11.389	11.688	11.018	11.299	11.581	11.235	11.516	11.798
B29	11.032	11.331	11.627	10.964	11.242	11.521	11.179	11.457	11.735
B30	11.103	11.397	11.689	11.128	11.414	11.698	11.349	11.635	11.920
B31	10.939	11.211	11.488	11.198	11.488	11.777	11.421	11.711	12.000
B32	10.819	11.083	11.354	11.113	11.399	11.685	11.335	11.621	11.908
B33	10.099	10.305	10.529	10.763	11.039	11.315	10.990	11.266	11.543
B34	10.105	10.311	10.537	10.768	11.048	11.329	10.997	11.278	11.559
B35	10.157	10.365	10.591	10.832	11.108	11.384	11.062	11.338	11.615
B36	10.112	10.319	10.542	10.780	11.053	11.327	11.007	11.281	11.554
B37	10.812	11.093	11.371	10.814	11.083	11.352	11.024	11.292	11.561
B38	10.943	11.238	11.528	10.877	11.151	11.425	11.088	11.362	11.636
B39	11.321	11.619	11.919	11.462	11.762	12.064	11.685	11.986	12.288

TABLE XI
LMPS FOR NODAL REACTIVE POWERS IN DIFFERENT SCENARIOS ($/MVARH)

Bus	s1	s2	s3	s4	s5	s6	s7	s8	s9
B1	-0.0195	-0.0159	-0.0127	-0.0136	-0.0119	-0.0084	-0.0132	-0.0113	-0.0089
B2	-0.0741	-0.0615	-0.0511	-0.0700	-0.0657	-0.0559	-0.0681	-0.0629	-0.0567
B3	-0.0357	-0.0288	-0.0227	-0.0235	-0.0199	-0.0131	-0.0231	-0.0190	-0.0141
B4	0.0205	0.0260	0.0312	0.0200	0.0237	0.0286	0.0203	0.0241	0.0284
B5	0.0216	0.0259	0.0302	0.0189	0.0222	0.0261	0.0192	0.0226	0.0262
B6	0.0173	0.0211	0.0250	0.0145	0.0175	0.0210	0.0147	0.0178	0.0212
B7	0.0343	0.0391	0.0439	0.0307	0.0345	0.0388	0.0311	0.0350	0.0392
B8	0.0367	0.0415	0.0463	0.0329	0.0367	0.0409	0.0333	0.0372	0.0413
B9	-0.0013	-0.0005	0.0003	-0.0062	-0.0057	-0.0053	-0.0068	-0.0062	-0.0058
B10	0.0000	0.0000	0.0000	0.0000	0.0000	0.0000	0.0000	0.0000	0.0000
B11	0.0091	0.0106	0.0122	0.0078	0.0090	0.0104	0.0079	0.0092	0.0105
B12	0.0237	0.0258	0.0280	0.0225	0.0242	0.0262	0.0229	0.0246	0.0265
B13	0.0090	0.0103	0.0116	0.0073	0.0081	0.0092	0.0073	0.0082	0.0091
B14	0.0243	0.0285	0.0322	0.0177	0.0201	0.0232	0.0175	0.0200	0.0228
B15	0.0459	0.0517	0.0569	0.0340	0.0372	0.0412	0.0334	0.0367	0.0403
B16	0.0189	0.0230	0.0266	0.0128	0.0150	0.0179	0.0122	0.0145	0.0171
B17	-0.0283	-0.0273	-0.0258	-0.0029	-0.0006	0.0031	-0.0042	-0.0017	0.0014
B18	-0.0308	-0.0277	-0.0244	-0.0083	-0.0054	-0.0003	-0.0091	-0.0059	-0.0020
B19	0.0059	0.0063	0.0068	0.0067	0.0071	0.0077	0.0069	0.0073	0.0079
B20	0.0155	0.0163	0.0172	0.0169	0.0178	0.0187	0.0173	0.0182	0.0191
B21	0.0186	0.0212	0.0236	0.0167	0.0185	0.0207	0.0168	0.0186	0.0207
B22	0.0000	0.0000	0.0000	0.0000	0.0000	0.0000	0.0000	0.0000	0.0000
B23	0.0093	0.0103	0.0113	0.0095	0.0105	0.0115	0.0099	0.0109	0.0119
B24	0.0130	0.0164	0.0195	0.0078	0.0096	0.0122	0.0073	0.0093	0.0115
B25	-0.0485	-0.0264	-0.0091	-0.0377	-0.0269	-0.0088	-0.0310	-0.0187	-0.0086
B26	-0.0599	-0.0598	-0.0595	-0.0570	-0.0575	-0.0572	-0.0594	-0.0598	-0.0594
B27	-0.0393	-0.0384	-0.0371	-0.0249	-0.0237	-0.0214	-0.0268	-0.0255	-0.0233
B28	-0.0338	-0.0335	-0.0330	-0.0325	-0.0325	-0.0321	-0.0335	-0.0334	-0.0329
B29	-0.0181	-0.0178	-0.0174	-0.0175	-0.0173	-0.0170	-0.0179	-0.0177	-0.0173
B30	-0.0719	-0.0597	-0.0496	-0.0679	-0.0638	-0.0543	-0.0661	-0.0611	-0.0551
B31	0.0155	0.0191	0.0226	0.0130	0.0158	0.0190	0.0133	0.0161	0.0192
B32	0.0000	0.0000	0.0000	0.0000	0.0000	0.0000	0.0000	0.0000	0.0000
B33	0.0000	0.0000	0.0000	0.0000	0.0000	0.0000	0.0000	0.0000	0.0000
B34	0.0000	0.0000	0.0000	0.0000	0.0000	0.0000	0.0000	0.0000	0.0000
B35	0.0000	0.0000	0.0000	0.0000	0.0000	0.0000	0.0000	0.0000	0.0000
B36	0.0000	0.0000	0.0000	0.0000	0.0000	0.0000	0.0000	0.0000	0.0000
B37	-0.0422	-0.0190	-0.0008	-0.0312	-0.0195	-0.0004	-0.0238	-0.0107	0.0000
B38	0.0000	0.0000	0.0000	0.0000	0.0000	0.0000	0.0000	0.0000	0.0000
B39	0.0000	0.0000	0.0000	0.0000	0.0000	0.0000	0.0000	0.0000	0.0000

the expense of higher corresponding PVC costs. Hence, the proposed model offers an optimal decision making tool for system operators, which makes a compromise between preserving a secure operating point and the imposed control costs.

REFERENCES

[1] M. Ortega-Vazquez and D. Kirschen, "Assessing the impact of wind power generation on operating costs," *IEEE Transactions on Smart Grid*, vol. 1, no. 3, pp. 295–301, 2010.

[2] A. Saber and G. Venayagamoorthy, "Efficient utilization of renewable energy sources by gridable vehicles in cyber-physical energy systems," *Systems Journal, IEEE*, vol. 4, no. 3, pp. 285 –294, sept. 2010.

[3] E. Vittal and A. Keane, "Identification of critical wind farm locations for improved stability and system planning," *Power Systems, IEEE Transactions on*, vol. 28, no. 3, pp. 2950–2958, Aug 2013.

[4] A. Rabiee, A. Soroudi, B. Mohammadi-Ivatloo, and M. Parniani, "Corrective voltage control scheme considering demand response and stochastic wind power," *Power Systems, IEEE Transactions on*, vol. 29, no. 6, pp. 2965–2973, Nov 2014.

[5] Z. Feng, V. Ajjarapu, and D. Maratukulam, "A comprehensive approach for preventive and corrective control to mitigate voltage collapse," *IEEE Transactions on Power Systems*, vol. 15, no. 2, pp. 791 –797, may 2000.

[6] W. Rosehart, C. Canizares, and V. Quintana, "Multiobjective optimal power flows to evaluate voltage security costs in power networks," *IEEE Transactions on Power Systems*, vol. 18, no. 2, pp. 578–587, 2003.

[7] S. Muyeen, R. Takahashi, and J. Tamura, "Operation and control of hvdc-connected offshore wind farm," *IEEE Transactions on Sustainable Energy*, vol. 1, no. 1, pp. 30–37, April 2010.

[8] A. Almeida, E. Valenca de Lorenci, R. Coradi Leme, A. Zambroni de Souza, B. Lima Lopes, and K. Lo, "Probabilistic voltage stability assessment considering renewable sources with the help of the pv and qv curves," *Renewable Power Generation, IET*, vol. 7, no. 5, pp. 521–530, Sept 2013.

[9] E. Haesen, C. Bastiaensen, J. Driesen, and R. Belmans, "A probabilistic formulation of load margins in power systems with stochastic generation," *Power Systems, IEEE Transactions on*, vol. 24, no. 2, pp. 951–958, May 2009.

[10] R. Bessa, M. Matos, I. Costa, L. Bremermann, I. Franchin, R. Pestana, N. Machado, H. Waldl, and C. Wichmann, "Reserve setting and steady-state security assessment using wind power uncertainty forecast: A case study," *IEEE Transactions on Sustainable Energy*, vol. 3, no. 4, pp. 827–836, Oct 2012.

[11] A. Tamimi, A. Pahwa, and S. Starrett, "Effective wind farm sizing method for weak power systems using critical modes of voltage instability," *Power Systems, IEEE Transactions on*, vol. 27, no. 3, pp. 1610–1617, Aug 2012.

[12] S. Bu, W. Du, and H. Wang, "Probabilistic analysis of small-signal rotor angle/voltage stability of large-scale ac/dc power systems as affected by grid-connected offshore wind generation," *Power Systems, IEEE Transactions on*, vol. 28, no. 4, pp. 3712–3719, Nov 2013.

[13] V. Kumar, K. Reddy, and D. Thukaram, "Coordination of reactive power in grid-connected wind farms for voltage stability enhancement," *Power Systems, IEEE Transactions on*, vol. 29, no. 5, pp. 2381–2390, Sept 2014.

[14] M. Montilla-DJesus, D. Santos-Martin, S. Arnaltes, and E. Castronuovo, "Optimal reactive power allocation in an offshore wind farms with lcc-hvdc link connection," *Renewable Energy*, 2011.

[15] ——, "Optimal operation of offshore wind farms with line-commutated hvdc link connection," *Energy Conversion, IEEE Transactions on*, vol. 25, no. 2, pp. 504–513, June 2010.

[16] P. Kundur, *Power system stability and control*. McGraw-Hill Education (India) Pvt Ltd, 1994.

[17] K. Tomsovic, "Integrated security analysis," *Final Report. Power Systems Engineering Research Center (PSERC) Publication*, pp. 03–06, 2004.

[18] V. Ajjarapu and A. P. S. Meliopoulos, *Preventing Voltage Collapse with Protection Systems that Incorporate Optimal Reactive Power Control*. Final Project Report PSERC Publication 08-20, Oct 2008.

[19] Y. Ben-Haim, *Info-gap decision theory: decisions under severe uncertainty*. Academic Press, 2006.

[20] A. Soroudi and M. Ehsan, "Igdt based robust decision making tool for dnos in load procurement under severe uncertainty," *Smart Grid, IEEE Transactions on*, vol. 4, no. 2, pp. 886–895, June 2013.

[21] F. N. Regression, "Fuzzy mathematics in economics and engineering," 2002.

[22] A. Soroudi and T. Amraee, "Decision making under uncertainty in energy systems: State of the art," *Renewable and Sustainable Energy Reviews*, vol. 28, pp. 376–384, 2013.

[23] R. Rockafellar and S. Uryasev, "Conditional value-at-risk for general loss distributions," *Journal of Banking & Finance*, vol. 26, no. 7, pp. 1443 – 1471, 2002.

[24] A. J. Conejo, M. Carrión, and J. M. Morales, *Decision making under uncertainty in electricity markets*. Springer, 2010, vol. 1.

[25] A. Rabiee, M. Parvania, M. Vanouni, M. Parniani, and M. Fotuhi-Firuzabad, "Comprehensive control framework for ensuring loading margin of power systems considering demand-side participation," *Generation, Transmission Distribution, IET*, vol. 6, no. 12, pp. 1189–1201, December 2012.

[26] I. El-Samahy, K. Bhattacharya, C. Canizares, M. Anjos, and J. Pan, "A procurement market model for reactive power services considering system security," *Power Systems, IEEE Transactions on*, vol. 23, no. 1, pp. 137–149, Feb 2008.
[27] A. Rabiee and A. Soroudi, "Stochastic multiperiod opf model of power systems with hvdc-connected intermittent wind power generation," *Power Delivery, IEEE Transactions on*, vol. 29, no. 1, pp. 336–344, Feb 2014.
[28] R. J. Avalos, C. A. Cañizares, F. Milano, and A. J. Conejo, "Equivalency of continuation and optimization methods to determine saddle-node and limit-induced bifurcations in power systems," *IEEE Transactions on Circuits and Systems-I*, vol. 56, no. 1, pp. 210–223, 2009.
[29] K. Burman, D. Olis, V. Gevorgian, A. Warren, R. Butt, P. Lilienthal, and J. Glassmire, "Integrating renewable energy into the transmission and distribution system of the us virgin islands," National Renewable Energy Laboratory (NREL), Golden, CO., Tech. Rep., 2011.
[30] A. Soroudi and A. Rabiee, "Optimal multi-area generation schedule considering renewable resources mix: a real-time approach," *Generation, Transmission Distribution, IET*, vol. 7, no. 9, pp. 1011–1026, Sept 2013.
[31] R. Zimmerman, C. Murillo-Sanchez, and R. Thomas, "Matpower: Steady-state operations, planning, and analysis tools for power systems research and education," *Power Systems, IEEE Transactions on*, vol. 26, no. 1, pp. 12–19, Feb 2011.
[32] A. Conejo, F. Milano, and R. Garcia-Bertrand, "Congestion management ensuring voltage stability," *Power Systems, IEEE Transactions on*, vol. 21, no. 1, pp. 357–364, Feb 2006.
[33] X.-Y. Ma, Y.-Z. Sun, H.-L. Fang, and Y. Tian, "Scenario-based multi-objective decision-making of optimal access point for wind power transmission corridor in the load centers," *IEEE Transactions on Sustainable Energy*, vol. 4, no. 1, pp. 229–239, Jan 2013.
[34] A. Soroudi and M. Afrasiab, "Binary pso-based dynamic multi-objective model for distributed generation planning under uncertainty," *Renewable Power Generation, IET*, vol. 6, no. 2, pp. 67–78, March 2012.
[35] P. E. Gill, W. Murray, and M. A. Saunders, "Snopt: An SQP algorithm for large-scale constrained optimization," *SIAM Review*, vol. 47, no. 1, pp. 99–131, 2005.
[36] A. Soroudi, M. Ehsan, R. Caire, and N. Hadjsaid, "Hybrid immune-genetic algorithm method for benefit maximisation of distribution network operators and distributed generation owners in a deregulated environment," *Generation, Transmission & Distribution, IET*, vol. 5, no. 9, pp. 961–972, 2011.

Abbas Rabiee (M14) Received the B.Sc. degree in electrical engineering from Iran University of Science and Technology (IUST), Tehran, in 2006, and the M.Sc. and Ph.D. degrees in electrical power engineering from Sharif University of Technology (SUT), Tehran, Iran, in 2008 and 2013, respectively. Currently, he is an Assistant Professor at the Department of Electrical Engineering, Faculty of Engineering, University of Zanjan, Zanjan, Iran. His research interests include power system operation and security, renewable energies, and the application of optimization techniques in power system operation.

Alireza Soroudi (M14) Received the B.Sc. and M.Sc. degrees from Sharif University of Technology, Tehran, Iran, in 2002 and 2004, respectively, both in electrical engineering. and Ph.D. degree from Grenoble Institute of Technology (Grenoble-INP), Grenoble, France, in 2011. He is the winner of the ENRE Young Researcher Prize at the INFORMS 2013. He is currently a senior researcher with the School of Electrical, Electronic, and Mechanical Engineering, University College Dublin with research interests in uncertainty modeling and optimization techniques applied to Smart grids, power system planning and operation.

Andrew Keane Andrew Keane (S04M07-SM'14) received the B.E. and Ph.D. degrees in electrical engineering from University College Dublin, Ireland, in 2003 and 2007, respectively. He is currently a Senior Lecturer with the School of Electrical, Electronic, and Communications Engineering, University College Dublin. He has previously worked with ESB Networks, the Irish Distribution System Operator. His research interests include power systems planning and operation, distributed energy resources, and distribution networks.